

Phase locking of coupled lasers with many longitudinal modes

Moti Fridman, Micha Nixon, Eitan Ronen, Asher A. Friesem and Nir Davidson

Dept. of Physics of Complex Systems, Weizmann Institute of Science, Rehovot 76100, Israel

Compiled May 24, 2022

Detailed experimental and theoretical investigations on two coupled fiber lasers, each with many longitudinal modes, reveal that the behavior of the longitudinal modes depends on both the coupling strength as well as the detuning between them. For low to moderate coupling strength only longitudinal modes which are common for both lasers phase-lock while those that are not common gradually disappear. For larger coupling strengths, the longitudinal modes that are not common reappear and phase-lock. When the coupling strength approaches unity the coupled lasers behave as a single long cavity with correspondingly denser longitudinal modes. Finally, we show that the gradual increase in phase-locking as a function of the coupling strength results from competition between phase-locked and non phase-locked longitudinal modes. © 2022 Optical Society of America

Phase locking of two coupled lasers operating with only one longitudinal mode was investigated over the years [1–4]. It was shown theoretically and experimentally that a simple relation exist between the coupling strength that is needed for phase locking and the frequency detuning between the lasers [4–6]. While a sharp transition from no phase locking to full phase locking when the coupling strength exceeds a critical value is predicted, the experimental results revealed a gradual transition, which could be explained by introducing noise to each laser [4, 6]. For lasers with many longitudinal modes it was shown that for strong coupling strength only common longitudinal modes survive, leading to full phase locking [7–10]. Yet, the detailed behavior of phase locking and the spectrum of longitudinal modes as a function of the coupling strength between coupled lasers were so far not reported.

Here we present our investigations and results on two coupled fiber lasers, each operating with up to 20,000 longitudinal modes. Specifically, we show how the phase locking between the two lasers and their longitudinal mode spectrum vary as a function of the coupling strength which is continually and accurately controlled with polarization elements. We find a gradual increase in the number of longitudinal modes which are phase locked as the coupling strength increases, leading to a gradual transition from no phase locking to full phase locking without the need to introduce noise. We support the experimental results with calculations in which a modified effective reflectivity model is exploited.

The experimental configuration for determining the phase locking and the spectrum of longitudinal modes for two coupled fiber lasers as a function of the coupling strength between them is presented in Fig. 1. Each fiber laser was comprised of a polarization maintaining Ytterbium doped fiber, where one end was attached to a high reflection fiber Bragg grating (FBG), with a central wavelength of $1064nm$ and a bandwidth of about $1nm$, that served as a back reflector mirror, the other end attached to a collimating graded index (GRIN) lens with anti-reflection coating to suppress any reflections back

into the fiber cores, and an output coupler (OC) with reflectivity of 20% common to both lasers. The lasers were pumped with $915nm$ diode lasers from the back end through the FBG. The two fiber lasers were forced to operate in orthogonal polarizations by using a calcite beam-displacer in front of a common output coupler and the coupling strength κ between the lasers was controlled by an intra-cavity quarter wave plate (QWP). $\kappa = \sin^2(2\theta)$, with θ the orientation of the QWP with respect to the calcite main axes. The optical length of the cavity of one fiber laser was $10m$ while the optical length of the other was $11.5m$, so each fiber has $\sim 20,000$ longitudinal modes within the FBG bandwidth. The combined output power was detected by fast photo detector which was connected to a RF spectrum analyzer, to measure the beating frequencies and determine the longitudinal mode spectrum at the output [5]. We also measured the phase locking between the two fiber lasers by detecting the interference of small part of the light from each laser with a CCD camera, and determining the fringe visibility [6]. The longitudinal mode spectrum was measured at first when $\theta = 0$ ($\kappa = 0$) and then sequentially repeated such measurement, each after rotating the QWP by 1° until we reached 45° ($\kappa = 1$).

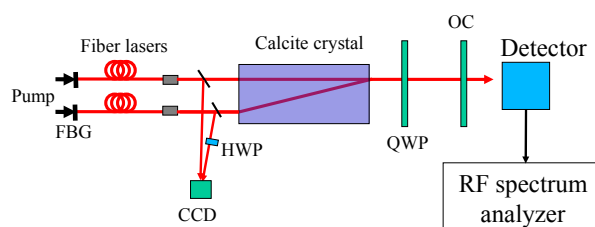


Fig. 1. Experimental configuration for investigating the phase locking and the spectrum of longitudinal modes of two coupled fiber lasers as a function of the coupling strength. FBG - fiber Bragg grating. HWP - half wave plate. QWP - quarter wave plate. OC - output coupler.

We developed a model for calculating the distribution of longitudinal modes and phase locking for the two

coupled lasers. For each laser, the effective reflectivity [11, 12] of its own reflection and the light coupled into it from the other laser was calculated self consistently. The longitudinal mode spectrum was then derived from the total effective reflectivity of the two lasers. The effective reflectivity resulting from the coupling to the other laser for each laser can be shown to be,

$$R_{1,2}^{eff} = \left(1 - r(1 - \sqrt{\kappa}) - \frac{r^2 \kappa e^{i l_{2,1} k}}{1 - r(1 - \sqrt{\kappa}) e^{i l_{2,1} k}} \right)^{-1}, \quad (1)$$

where k denotes the propagation vector of the light, κ the coupling strength between the two lasers, $l_{2,1}$ the length of each laser and r the reflectivity of the output coupler. To account for gain competition between the longitudinal modes we used $r = 0.55$ as a fitting parameter, rather than our experimental value of $r = 0.2$ [11]. We then sum over the round trip propagations to obtain the self consistent field for each laser as,

$$R_j^{eff} e^{i k l_j} + \left(R_j^{eff} e^{2 i k l_j} \right)^2 + \dots = \left(1 - R_j^{eff} e^{i k l_j} \right)^{-1}, \quad (2)$$

where $j = 1, 2$. Finally, the output laser field of the two coupled lasers R_{out} , namely the amplitude of the longitudinal modes, is obtained as a sum of the two self consistent fields, as

$$R_{out} = \left(1 - R_1^{eff} e^{i k l_1} \right)^{-1} + \left(1 - R_2^{eff} e^{i k l_2} \right)^{-1}. \quad (3)$$

Figure 2 shows the experimental and calculated longitudinal mode spectrum as a function of coupling strength κ . Figure 2(a) shows the experimental results of the longitudinal mode spectrum as a function of coupling strength over 200MHz range, and Fig. 2(b) the corresponding calculated results. Note that within our 1nm laser bandwidths, the 200MHz range would be repeated many times. The experimental and calculated results are also shown in greater detail for four specific coupling strengths ($\kappa = 0, 0.28, 0.7, \text{and } 1$) in Figs. 2(c)-(f), respectively. Without coupling (i.e. $\kappa = 0$) two independent sets of frequency combs exist simultaneously, one corresponds to the 10m long fiber laser (15MHz separation between adjacent longitudinal mode) while the other corresponds to the 11.5m long fiber laser (13MHz separation), as also seen in Fig. 2(c). Each 7th longitudinal mode of the 10m long laser is very close to the 8th mode of the other, so they are essentially common longitudinal modes. When κ is increased from 0 to 0.3 the longitudinal modes that are not common gradually disappear according to their detuning while transferring their energy to the remaining ones via the homogenous broadening of the gain. The longitudinal modes with the larger detuning disappear first while the ones with smaller detuning disappear for larger values of κ and only the common longitudinal mode remains, as also seen in Fig. 2(d), indicating that at this coupling strength there is full phase locking. As the coupling strength increases above 0.3 the longitudinal modes gradually reappeared,

as also seen in Fig. 2(e). The longitudinal modes with the smaller detuning reappear first and the ones with larger detuning reappear for larger values of κ . Finally, when κ approaches unity, whereby all the light from one laser is transferred to the other, new longitudinal modes appear in between adjacent longitudinal modes, as also seen in Fig. 2(f), corresponding to a single combined laser cavity whose length is the sum of the two lasers.

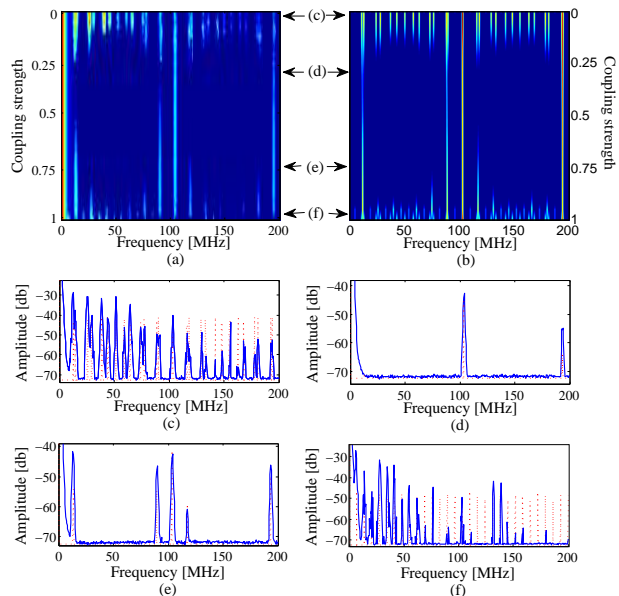


Fig. 2. Experimental and calculated distributions of longitudinal modes for two coupled lasers as a function of the coupling strength κ . (a) Experimental results; (b) calculated results; (c) $\kappa = 0$; (d) $\kappa = 0.28$; (e) $\kappa = 0.7$; (f) $\kappa = 1$. Solid (blue) curves denote experimental results and dotted (red) curves denote calculated results.

Figure 2 reveals a good quantitative agreement between the experimental and calculated results. In particular, the observed gradual disappearance of non-common longitudinal modes as the coupling is increased, their gradual reappearance when the coupling is further increased and finally the doubling of the frequency comb at near unity coupling strength are all accurately reconstructed by our model.

The results of Fig. 2 can be exploited to produce the full phase diagram of the longitudinal modes behavior, as shown in Fig. 3. Here the behavior is presented as a function of the coupling strength between the lasers and the detuning between adjacent longitudinal modes. The phase diagram includes four regions. In the first region of weak coupling the longitudinal modes are not phase locked for any finite detuning between them. In the second region of moderate to strong coupling and small detuning, the longitudinal modes are phase locked, indicating that the coupling is strong enough to overcome the detuning. In the third region where the coupling strengths is not sufficient to overcome the larger detuning between adjacent longitudinal modes, these modes

cannot lase. Finally, in the fourth region, where the coupling strength approaches unity, the two coupled lasers behave as a single and longer laser with denser longitudinal modes. As seen, for detuning smaller than about 1MHz there is a direct transition from no phase locking to phase locking as the coupling strength is increased. For larger detunings the transition from no phase locking to phase locking is interrupted by the no lasing region.

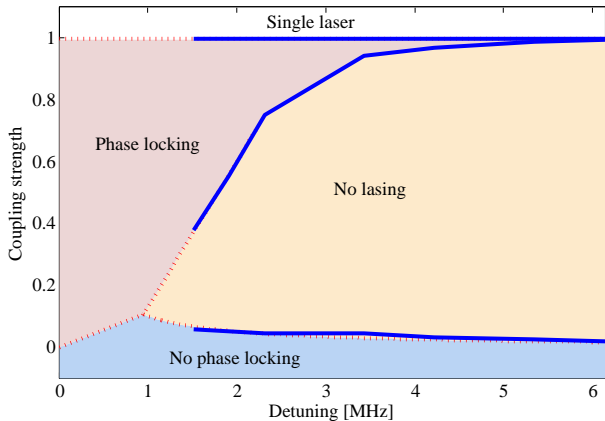


Fig. 3. Experimental and calculated phase diagram of the longitudinal modes behavior as a function of the coupling strength between two coupled lasers and detuning between adjacent longitudinal modes. Solid curves denote experimental results. Dotted curves denote calculated results.

We also measured directly the phase locking (i.e. fringe visibility) between the two coupled lasers as a function of the coupling strength. The results, presented in Fig. 4, reveal a gradual increase in phase locking as the coupling strength become stronger. Fig. 4 also shows the ratio of the power in the common longitudinal mode over that of all longitudinal modes for each coupling strength, measured from the results of Fig. 2(a). The good agreement between this ratio and the direct measure of phase locking verifies that the gradual increase in phase locking corresponds to the gradual disappearance of the non-common longitudinal modes which are not phase-locked. Finally, Fig. 4 also shows the ratio of the power in the common longitudinal mode over that of all longitudinal modes for each coupling strength, calculated from the results of Fig. 2(b) which are also in good agreement with both measurements.

To conclude, we presented how phase locking between two coupled lasers which operate with many longitudinal modes depends on the coupling strength and the detuning between the modes. We found that there is a gradual transition from no phase locking to full phase locking with increasing coupling strength due to the gradual disappearance of longitudinal modes that are not phase locked. The experimental results were confirmed with calculations using a modified effective reflectivity model for coupled lasers that we developed. Our results provide a fairly complete picture for elucidating the behavior of

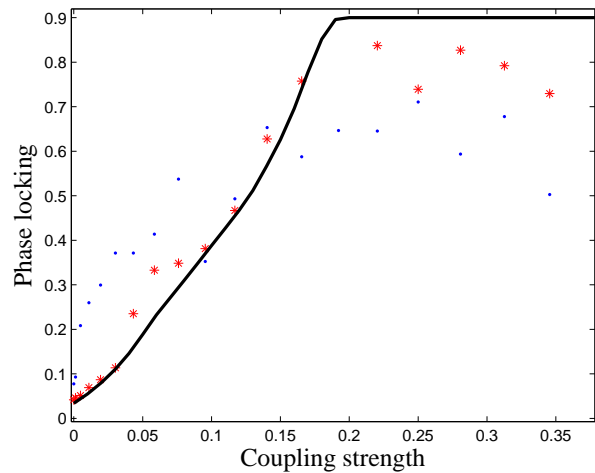


Fig. 4. Experimental and calculated phase locking as a function of the coupling strength between two coupled fiber lasers. Dots denote the directly measured phase locking; stars denote the phase locking calculated from experimental results in Fig 2(a); solid curve denotes the phase locking calculated from the results in Fig. 2(b).

the spectrum of the longitudinal modes in coupled lasers and its effect on phase locking.

This research was supported in part by the USA-Israel Binational Science Foundation.

References

1. R. Roy and K. S. Thornburg, Jr., "Experimental synchronization of chaotic lasers", *Phys. Rev. Lett.* **72**, 2009, (1997).
2. A. F. Glova, *Quantum Electron.* **33**, 283, (2003).
3. T. Y. Fan, *IEEE J. Sel. Top. Quantum Electron.* **11**, 567, (2005).
4. L. Fabiny, P. Colet, R. Roy, D. Lensta, *Phys. Rev. A.* **47**, 4287, (1993).
5. M. Fridman, V. Eckhouse, N. Davidson, and A. A. Friesem, *Opt. Lett.* **32**, 790, (2007).
6. V. Eckhouse, M. Fridman, N. Davidson, and A. A. Friesem, *Phys. Rev. Lett.* **100**, 024102, (2008).
7. M. Nakamura, K. Aiki, N. Chinone, R. Ito, and J. Umeda, *J. Appl. Phys.* **49**, 4644, (1978).
8. A. Shirakawa, T. Saitou, T. Sekiguchi, K.-i Ueda, *Opt. Lett.* **10**, 1167, (1999).
9. A. Shirakawa, K. Matsuo, and K.-i. Ueda, *Proc. SPIE* **5662**, 482, (2004).
10. J. E. Rothenberg, *Optical Fiber Communication Conference (OFC)* San Diego, California March 22, (2009).
11. S. S. Cohen, V. Eckhouse, A. A. Friesem, N. Davidson, *Opt. Comm.* **282**, 1861, (2009).
12. A. E. Siegman, "Lasers" (University Science Books, Mill Valley, California) 1986, Chap. 11.